Evaluation of Poloidal Distribution from Edge Impurity Emissions Measured at Different Toroidal Positions in Large Helical Device*)

Hongming ZHANG[1)], Shigeru MORITA[1,2)], Tetsutarou OISHI[1,2)], Masahiro KOBAYASHI[1,2)], Motoshi GOTO[1,2)] and Xianli HUANG[1)]

[1)]*Graduate University for Advanced Studies, Toki, Gifu 509-5292, Japan*
[2)]*National Institute for Fusion Science, Toki, Gifu 509-5292, Japan*

(Received 24 November 2014 / Accepted 26 February 2015)

Two-dimensional (2-D) distribution of edge impurity line emissions has been measured for CIV, CVI, FeXV and FeXVIII using a space-resolved extreme ultraviolet (EUV) spectrometer in Large Helical Device (LHD). The top and the bottom edges of the distribution show a strong emission trajectory along the plasma boundary. In this study, the poloidal distribution of the impurity emissivity is evaluated by analyzing the 2-D distribution against magnetic flux surfaces calculated with a three-dimensional (3-D) equilibrium code, i.e., VMEC. The inner and outer boundaries of the edge impurity locations are estimated by analyzing the vertical profile of each impurity emission measured at different toroidal positions. The observation chord length passing through an emission contour is calculated on the basis of the radial thickness of the impurity emission location. The poloidal distributions of CIV, CVI, FeXV and FeXVIII with different ionization energies are thus reconstructed from their 2-D distributions. A non-uniform poloidal distribution is clearly observed for each of these impurity species at different plasma radii. It is experimentally confirmed that the poloidal distribution becomes gradually uniform as the radial location of the impurity ions changes from the ergodic layer toward the plasma core. The non-uniform poloidal distribution of the CIV emissivity is further confirmed by a simulation with the 3-D edge transport code, EMC3-EIRENE.

Keywords: EUV spectroscopy, two-dimensional impurity distribution, ergodic layer, edge impurity emission, non-uniform poloidal distribution

DOI: 10.1585/pfr.10.3402038

1. Introduction

In the Large Helical Device (LHD), the core plasma is surrounded by the ergodic layer, in which magnetic fields with three-dimensional (3-D) structures are formed by higher-order components of the magnetic fields created by a pair of helical coils and by overlapping of edge small islands [1–3]. A two-dimensional (2-D) space-resolved extreme ultraviolet (EUV) spectrometer has been developed to measure the 2-D distribution of impurity line emissions in the ergodic layer [4]. The 2-D distributions of edge impurity emissions have been measured for various impurity species, e.g., CIV, HeII and FeXVI [4, 5]. An entirely non-uniform 2-D distribution has been observed for such edge impurity emissions. These impurity emissions are enhanced at the top and bottom plasma boundaries and in the vicinity of the X-points. Such measured 2-D distributions may reflect a non-uniform poloidal distribution of the edge impurity emissions. Therefore, evaluating the poloidal distribution of edge impurity emissions is important for deeper understanding of the impurity behavior at the plasma edge, in particular, in the ergodic layer. As the LHD plasma shape poloidally rotates five times during one toroidal turn, the poloidal distribution of the edge impurity emissions can be estimated from their 2-D distributions. In practice, the poloidal distribution of impurity emissivities is obtained by analyzing each vertical profile measured at different toroidal positions. In this study, the poloidal impurity distribution is presented for CIV, CVI, FeXV and FeXVIII with different ionization energies. The result is compared with simulation result of the EMC3-EIRENE code.

2. EUV Spectrometer and 2-D Impurity Emission Distribution Measurement

A 2-D space-resolved EUV spectrometer has been developed to measure the 2-D distribution of impurity emissions in the wavelength range of 60 to 400 Å by horizontally scanning the optical axis of the spectrometer [4]. Figure 1 shows the horizontal view of the LHD plasma with the ergodic layer. The position of the LHD port is shown by a diamond solid line. The observation area for the 2-D distribution measurement is limited to 120 cm and 90 cm in the vertical and horizontal directions, respectively. The inboard and outboard X-point trajectories are represented

author's e-mail: zhang.hongming@nifs.ac.jp
*) This article is based on the presentation at the 24th International Toki Conference (ITC24).

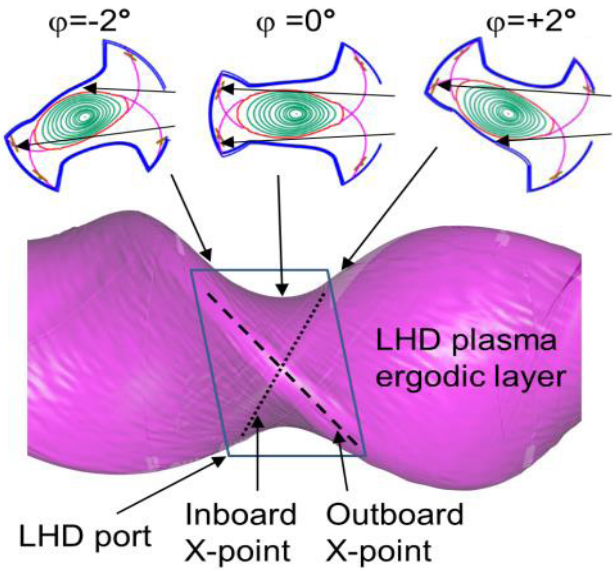

Fig. 1 Horizontal view of LHD ergodic layer and poloidal plasma cross-sections at three different toroidal angles $\varphi = -2°$, $0°$ and $+2°$.

by the dotted and dashed lines, respectively. The spatial resolutions of the space-resolved EUV spectrometer (at a horizontal scanning speed $V_{\mathrm{EUV}} = 0$) in the LHD vacuum vessel (at the major radius $R = 3.60$ m) are 65.3 mm and 30.2 mm in horizontal and vertical directions, respectively. The horizontal spatial resolution degrades a little when the horizontal scanning speed increases, e.g., 80 mm at $V_{\mathrm{EUV}} = 2.5$ mm/s [4].

The main impurity species in the LHD discharges is carbon which originates from the divertor plates made of graphite. The carbon density relative to the electron density ($n_{\mathrm{carbon}}/n_{\mathrm{e}}$) roughly ranges in $1\% \le n_{\mathrm{carbon}}/n_{\mathrm{e}} \le 3\%$. The iron impurity originates from the first wall made of stainless steel, and its density relative to the electron density, $n_{\mathrm{Fe}}/n_{\mathrm{e}}$, is usually very small, i.e., $n_{\mathrm{Fe}}/n_{\mathrm{e}} < 0.01\%$. As the magnetic field connection length in the ergodic layer of the LHD is longer compared with the case of tokamaks, friction force is dominant rather than the ion temperature gradient (ITG) force. Thus, the iron ion sputtered on the first wall tends to move toward the divertor plates. Therefore, in the LHD, the edge impurity transport does not depend on the impurity source location.

Figure 2 shows the 2-D distributions of the CIV (384.174 Å, 64.0 eV), CVI (2×33.73 Å, 490.0 eV), FeXV (284.164 Å, 456.2 eV) and FeXVIII (93.92 Å, 1357.8 eV) impurity emissions at the specified wavelengths and ionization energies. All of the 2-D distributions are measured during the flat-top phase of the ion cyclotron resonance frequency (ICRF) discharges at the magnetic-axis position of $R_{\mathrm{ax}} = 3.60$ m for similar plasma parameters, i.e., line-averaged electron density $n_{\mathrm{e}} \approx 1 \times 10^{13}$ cm^{-3}. No remarkable variation in any of the parameters is observed during the horizontal scanning. The intensities of the impurity line emissions are absolutely calibrated using radial pro-

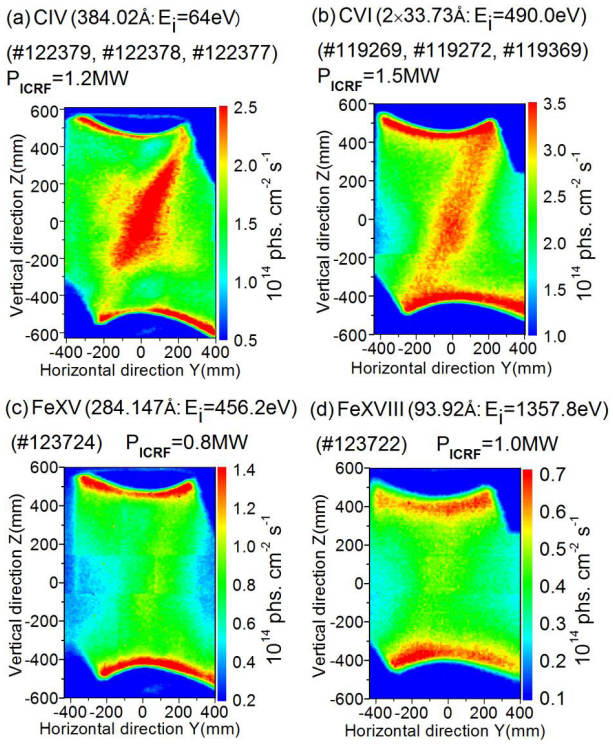

Fig. 2 2-D distributions of (a) CIV, (b) CVI, (c) FeXV and (d) FeXVIII at $R_{\mathrm{ax}} = 3.60$ m. The shot numbers and ICRF power are indicated in each distribution.

files of the bremsstrahlung continuum in the EUV and visible ranges [6]. In the measured 2-D distributions, the spectral intensities near the top and bottom plasma boundaries are seen to be enhanced because of a long chord length passing through the edge plasma. The inboard X-point trajectory (see Fig. 1) is also enhanced for CIV and CVI, indicating a non-uniform poloidal distribution in the ergodic layer.

3. Analysis of Poloidal Distribution

The elliptical cross sections of the LHD plasma at three different toroidal positions, i.e., $\varphi = -2°$, $0°$, and $+2°$, are shown in Fig. 1. The observation chords passing through the top and bottom plasma boundaries are also shown by two solid arrows in each poloidal cross section. In the figure, it is clear that the emission intensity at the top and bottom edges measured at different toroidal positions can show information on the poloidal distribution of impurity emissions. Thus, an evaluation of the poloidal distribution of the edge impurity emissions is attempted by analyzing the impurity emission at the top and bottom edges of the 2-D distributions. In the analysis, the data from the X-points with extremely non-uniform emissions are not used.

As the first step, the magnetic flux surface of LHD is calculated with a 3-D equilibrium code (VMEC) as a function of pressure profile. Although no magnetic surface exists in the ergodic layer, virtual magnetic surfaces, which

are calculated by extrapolating the magnetic flux surface at last closed flux surface (LCFS), are assumed at $\rho > 1$. This assumption is usually used when the edge plasma in the ergodic layer is analyzed in the LHD.

An example of the vertical profile of impurity emissions at the top edge is shown in Fig. 3 for CIV measured at $Y = 0$, which means $\varphi = 0°$ (see Fig. 2). A sharp peak is observed near the plasma edge boundary. Here, the inner and outer boundaries of the impurity vertical profile are defined by intensities at the peak and the half maximum, respectively. In the figure, the inner and outer boundaries of the CIV radial profiles are estimated to be $\rho = 1.02$ and $\rho = 1.06$, respectively.

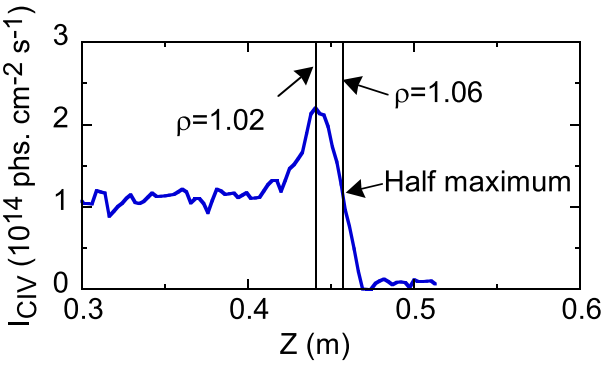

Fig. 3 CIV vertical profile at $Y = 0$ as a function of vertical position (also see Fig. 2).

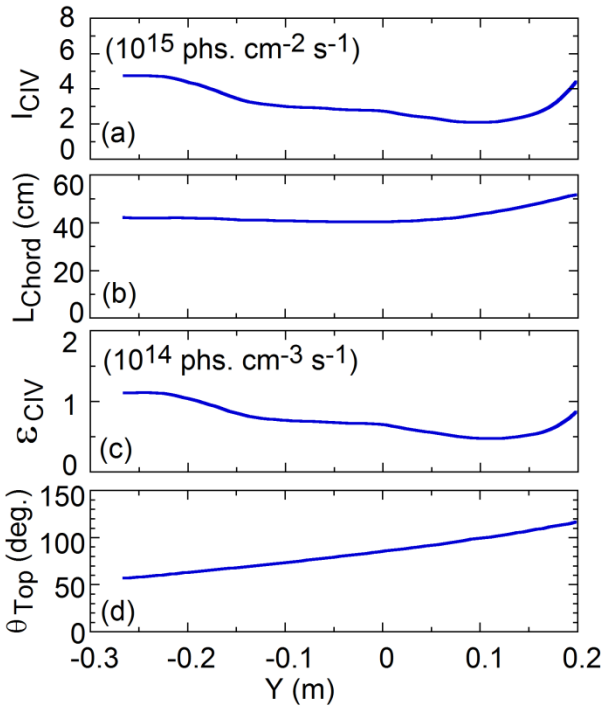

Fig. 4 (a) Chord-integrated intensity of CIV, (b) observation chord length, (c) CIV emissivity and (d) poloidal angle at the top plasma edge as a function of horizontal position Y.

After analyzing the inner and outer boundaries of impurity emissions, the chord-integrated intensity is estimated by integrating the emission between the two boundaries. Figure 4 (a) shows the chord-integrated intensity of CIV emissions at the top plasma edge, which is calculated as a function of the horizontal position. The observation chord length calculated at each toroidal position is shown in Fig. 4 (b). The local emissivity of CIV in each case is then obtained by dividing the chord-integrated intensity by the chord length. The results are plotted as shown in Fig. 4 (c).

The poloidal angle at the top plasma edge is calculated from the assumed magnetic flux surface in the ergodic layer for each horizontal position, as shown in Fig. 4 (d). Thus, the poloidal distribution of the CIV emissivity near the top edge can be reconstructed using vertical and horizontal coordinates from the 2-D CIV distribution. The poloidal distribution of the CIV emissivity near the bottom edge can also be analyzed in the same manner.

4. Results and Discussion

The poloidal emissivity distributions evaluated from the 2-D distributions in Figs. 2 (a) - (d) are shown in Figs. 5 (a) - (d) as a function of the poloidal angles θ_{Top} and θ_{Bottom} at the top and bottom edges, respectively. Here, the poloidal angle is defined as the angle toward the counterclockwise direction, with the reference as the point along

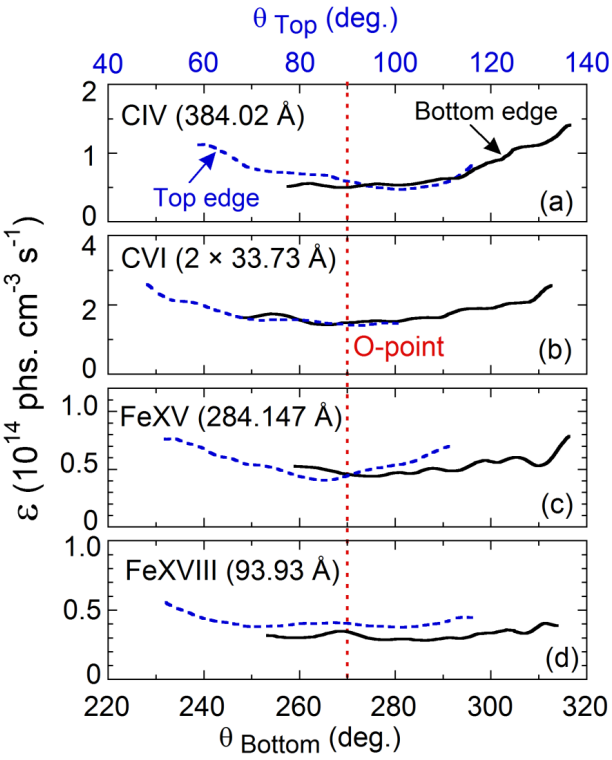

Fig. 5 Poloidal distributions of (a) CIV, (b) CVI, (c) FeXV and (d) FeXVIII as a function of poloidal angles θ_{Top} and θ_{Bottom}.

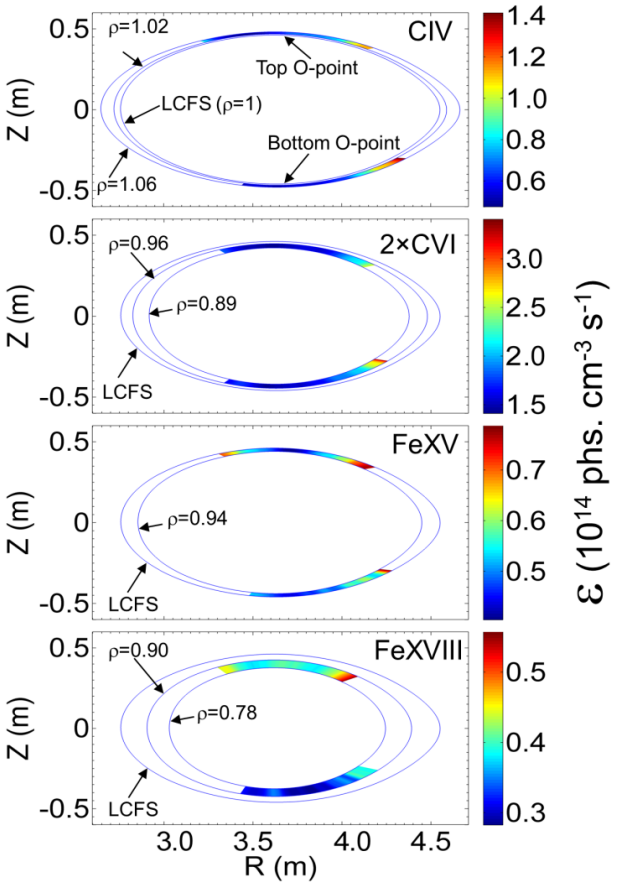

Fig. 6 Poloidal distributions of (a) CIV, (b) CVI, (c) FeXV and (d) FeXVIII at horizontally elongated plasma cross-sections. The measure of the emissivity is represented by different colors.

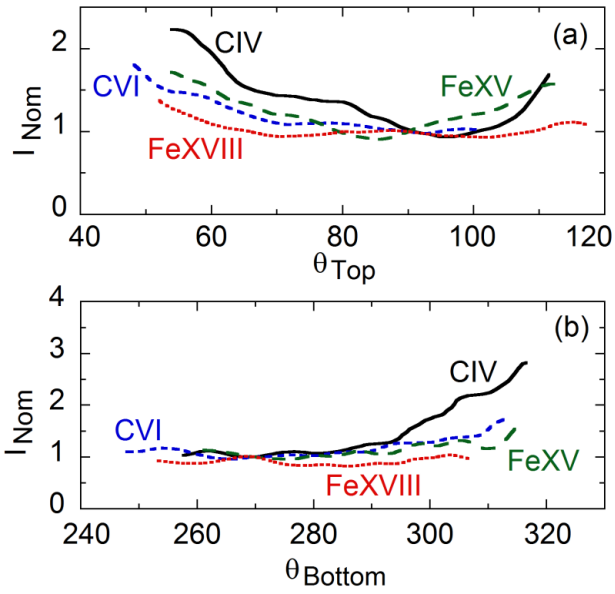

Fig. 7 Emissivity profiles of CIV, CVI, FeXV and FeXVIII at (a) top and (b) bottom regions normalized to the emissivity at $\theta_{\mathrm{Top}} = 90°$ and $\theta_{\mathrm{Bottom}} = 270°$, respectively.

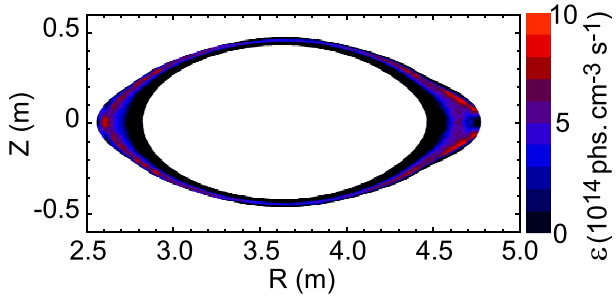

Fig. 8 Simulation of emissivity distribution of CIV (312.4 Å) using EMC3-EIRINE code under similar conditions as the experiment.

the axis of the elliptical plasma on the outboard side. The poloidal distributions measured at the top and bottom edges are plotted as the dashed and solid lines, respectively. Due to the limited observation range of the EUV spectrometer, the distributions are obtained in the ranges $55° \leq \theta_{\mathrm{Top}} \leq 110°$ and $255° \leq \theta_{\mathrm{Bottom}} \leq 320°$. The poloidal distributions of these impurity species are also plotted against the horizontally elongated plasma cross sections. The results shown in Fig. 6 indicate that the radial location of the impurity ions changes inwardly (toward the plasma center) as the ionization energy increases. From the Figs. 5 and 6, it is clear that the poloidal distribution is non-uniform for impurity ions existing in the ergodic layer and in the vicinity of the LCFS, and that the non-uniformity becomes stronger with a reduction in the ionization energy of the impurity ions. This means that impurity ions located at the outer region of the ergodic layer exhibit larger non-uniformity in the poloidal distribution. In addition, the emissivity becomes stronger as the impurity location gets closer to the X-point, whereas it is weak at both the top and the bottom O-points defined by the poloidal positions of the elliptical plasma boundary adjacent to the helical coils.

In order to compare in detail the non-uniformity among the four impurity species, the emissivity distributions from the top and bottom regions are normalized to the emissivity at the top ($\theta_{\mathrm{Bottom}} = 90°$) and bottom ($\theta_{\mathrm{Bottom}} = 270°$) O-points, respectively. The results for the top and bottom regions are shown in Figs. 7 (a) and (b), respectively. The normalized poloidal distribution becomes gradually uniform as the impurity ions radially move toward the plasma center. The poloidal profile of CIV shows an extremely non-uniform distribution. As the C^{3+} ions with low ionization energy ($E_{\mathrm{i}} = 64$ eV) are located near the edge boundary of the ergodic layer, they are strongly affected by a specific edge impurity transport, which is dominant in the ergodic layer with a 3-D magnetic field structure. On the contrary, the poloidal profile of FeXVIII located within $0.78 \leq \rho \leq 0.90$ indicates a relatively flat distribution. This means the FeXVIII emissivity is a function of the magnetic surface.

The carbon distribution in the ergodic layer has been also analyzed using the 3-D edge plasma transport code, EMC3-EIRINE [7]. The emissivity distribution of CIV (312.4 Å) simulated with the code is plotted in Fig. 8. The plotted results indicate that the CIV emission located in the ergodic layer is stronger when the radial location moves outside. The simulated result entirely supports our present result, despite the estimation of the poloidal distribution is obtained from the 2-D distribution. Therefore, the present analysis can provide a reliable method to evaluate the impurity poloidal distribution.

5. Summary

The poloidal emissivity distributions of CIV, CVI, FeXV and FeXVIII have been reconstructed from their 2-D distributions measured with the space-resolved EUV spectrometer in the LHD. A non-uniform poloidal distribution has been clearly observed for CIV, whereas the FeXVIII distribution is basically a function of the magnetic surface. The present CIV results are well supported by a 3-D simulation.

Acknowledgments

The authors thank all members of the LHD Experiment Group for their technical supports. This work was partially carried out under the LHD project financial support (NIFS14ULPP010) and also partly supported by the JSPS-NRF-NSFC A3 Foresight Program in the field of Plasma Physics (NSFC: No. 11261140328, NRF: No. 2012K2A2A6000443).

[1] N. Ohyabu *et al*., Nucl. Fusion **34**, 387 (1994).
[2] T. Morisaki *et al*., J. Nucl. Mater. **31**, 3548 (2003).
[3] S. Morita *et al*., Nucl. Fusion **53**, 093017 (2013).
[4] E.H. Wang *et al*., Rev. Sci. Instrum. **83**, 043503 (2012).
[5] S. Morita *et al*., Plasma Phys. Control. Fusion **56**, 094007 (2014).
[6] C.F. Dong *et al*., Rev. Sci. Instrum. **83**, 10D509 (2012).
[7] M. Kobayashi *et al.*, Nucl. Fusion **53**, 033011 (2013).